processes

MDPI

Article

Effects of Over-Sintering on Cyclic Calcination and Carbonization of Natural Limestone for CO_2 Capture

Jiangtao Chen [1], Jinxing Wang [2,*], Huawei Jiang [3], Xiangli Zuo [3] and Xin Yang [4]

[1] Henan Power Plant Energy Conservation and Environmental Protection Engineering Technology Research Center, Zhengzhou Electric Power College, Zhengzhou 450004, China; chenjt-1@163.com
[2] College of Civil and Architectural Engineering, North China University of Science and Technology, Tangshan 063210, China
[3] Institute of Energy Engineering, College of Mechanical and Electrical Engineering, Qingdao University, Qingdao 266071, China; jianghwwh@qdu.edu.cn (H.J.); zuoxiangli@qdu.edu.cn (X.Z.)
[4] School of Water Conservancy and Hydroelectric Power, Hebei University of Engineering, Handan 056002, China; yangxin890322@126.com
* Correspondence: wangruoguang860928@126.com

Abstract: To know the sustainable performance of calcium-based adsorbents is one of the important aspects to realize efficient and economical carbon capture, and to systematically study the properties of natural adsorbents is conducive to their industrialization. The cyclic calcination and carbonation characteristics of a typical natural limestone were investigated using a thermal gravimetric analyzer. Two kinds of over-sintering conditions were selected to emphatically study the cyclic separation of CO_2 from limestones through prolonging the calcination time and increasing the calcination temperature. The results showed that the untimely end of the chemical reaction control stage caused by excessive sintering is the direct reason for the reduction in cyclic carbonation conversion, and the changes in surface morphology of calcined products due to pore collapse and fusion are the fundamental reasons for the reduction in cyclic carbonation conversion. The excessive sintering caused by extending the calcining time or increasing the calcining temperature has great inhibition on this cycle only; the inhibition decreases rapidly in subsequent cycles. In addition, SEM and BET–BJH tests further confirm the influence of the over-sintering phenomenon. With the further increase in cycle number, the early excessive sintering has certain stimulative effects on the subsequent carbonation reaction. It is expected to provide a reference for the subsequent research and development of natural calcium-based adsorbents.

Keywords: calcium-based adsorbent; natural limestone; cyclic reaction; carbon capture; over-sintering

Citation: Chen, J.; Wang, J.; Jiang, H.; Zuo, X.; Yang, X. Effects of Over-Sintering on Cyclic Calcination and Carbonization of Natural Limestone for CO_2 Capture. *Processes* **2024**, *12*, 1926. https://doi.org/10.3390/pr12091926

Academic Editor: Paola Ammendola

Received: 5 August 2024
Revised: 1 September 2024
Accepted: 4 September 2024
Published: 7 September 2024

1. Introduction

Considering China's energy structure, which is rich in coal, poor in petroleum and low in natural gas, fossil energy will still play an important role in ensuring power supply and heat supply for some time in the future. However, the use of coal also leads to the emission of a large amount of polluting gases and greenhouse gases. To achieve China's target of peak carbon dioxide emissions and carbon neutrality, the combination of carbon capture, utilization and storage (CCUS) for coal-fired power is a potential technical path [1–3].

CCUS refers to the capture or separation of carbon dioxide from the emissions during industrial processes or energy production and the following utilization or transportation to appropriate sites for storage. In the carbon capture process, due to the low cost, widely available sources and considerable adsorption capacity, the carbonation reaction of calcium-based adsorbents, such as CaO absorpting CO_2 and the calcination reaction of $CaCO_3$, which could be circularly used, is a feasible technical route [4–7]. A calcium looping process can also be applied to many aspects, such as hydrogen production from natural gas

using steam reforming, hydrogen production by biomass gasification, thermochemical heat storage and gas–solid chemical heat pump systems [8–10].

At present, the cyclic calcination/carbonation reactions (CCCR) mainly use a dual-fluidized bed reactor as the mainstream reaction device, which is mainly composed of an absorption reactor and a calcination reactor and realizes the circulation exchange of Ca-based materials through intermediate connections, as shown in Figure 1. In the absorption reactor, CaO particles would react with CO_2 to produce $CaCO_3$ particles, which are transported into the calcination reactor for thermal decomposition to realize the regeneration of CaO particles. Regenerative CaO particles would then be returned to the absorption reactor again for recycling so as to achieve the absorption and release of CO_2. In this process, the limestone calcination reaction is the premise of the subsequent decarbonization reaction, and the decomposition degree due to the calcination reaction has a significant impact on CO_2 removal. In the calcination process of natural limestone, in the first stage, CO_2 is mainly decomposed by calcium carbonate at a high temperature, and many large pores are generated, while in the second stage, CO_2 is mainly adsorbed and chemically reacted with calcium oxide. If the pores become smaller after sintering at this time, it will inevitably affect the subsequent cycle performance.

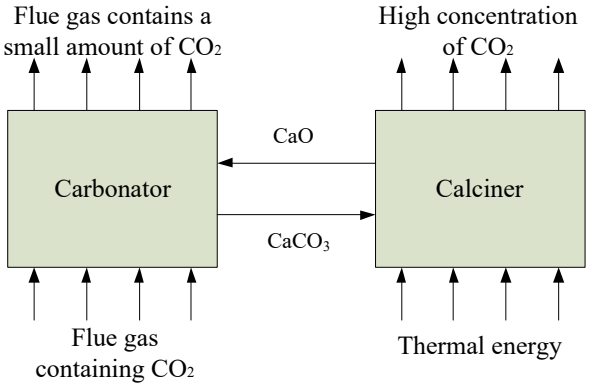

Figure 1. Simplified schematic diagram of the CCCR process in a dual-fluidized bed.

Since Shimizu [11] proposed the technology of using the calcium-based absorbent CCCR method to separate CO_2 in a dual-fluidized bed reactor, a significant amount of research has been carried out. In the process of calcium-based absorption CCCR technology, the pore structure of the calcined product directly determines the change in carbonation conversion rate and, at the same time, indirectly affects the macroscopic dynamic characteristics. The development of microstructure characteristics can provide a better understanding of the macroscopic reaction characteristics of the CCCR process and lay the foundation for the modification of calcium-based absorbents. At present, most studies have focused on the effect of the calcination temperature and particle size on the subsequent carbonation reaction, and the effect on excessive sintering of limestone needs to be further studied. Chen Hongwei [12] found that the kinetic parameters of the calcination reaction of pure $CaCO_3$ and limestone would vary with the change in calcination temperature, and the change rules of the two are different; however, the apparent activation energy and the pre-finger factor change with temperature are similar, and there is a kinetic compensation effect.

Li [13] studied the effect of carbonation temperature, calcination temperature and particle size on the conversion rates of carbonation during the limestone and dolomite CCCR process and found that, when the calcination temperature exceeds 1050 °C, the conversion rate of limestone carbonation attenuates sharply with the increase in the number of cycles, while the degree of attenuation of dolomite is not large, and the CO_2 absorption of dolomite is higher than that of limestone during calcination at high temperature. With the increase in the number of cyclic reactions, the microstructure of the limestone calcined product changes greatly, while the change in dolomite is small. At the same time, the accompanying chemical reaction can also include reforming methane to produce hydrogen [14],

biomass oil to produce hydrogen [15] and the modification [16] of the catalyst itself. In the method of catalyst modification, alkali metal modification [17] is considered to be a more promising method.

At present, the research hotspots of calcium-based adsorbents are mainly focused on the carbon capture characteristics of modified calcium-based adsorbents. Xu Yongqing [18] proposed to use a new hydration impregnation method to prepare K_2CO_3-modified calcium-based adsorbents and studied them using a simultaneous thermal analyzer. Kuang Shengduo [19] used the sol-gel self-propagating combustion method to prepare magnesium/yttrium (Mg/Y)-modified Ca-based adsorbents. The test proved that the cycle adsorption performance was improved, and the effect of Y doping was better than that of Mg. Considering that the current research is mainly focused on the effects of different types of modified calcium-based adsorbents, calcination temperature and particle size on the subsequent carbonation reaction, there are few studies on the over-sintering of calcium-based adsorbents. However, the sintering of calcium-based adsorbents is inevitable during operation. Therefore, in this paper, calcium-based adsorbents were over-sintered at different cycle times and temperatures to investigate the effects of over-sintering on the characteristics of calcium-based adsorbents for the cyclic separation of CO_2.

2. Experimental

2.1. System Device

This research was conducted using a self-built thermogravimetric analysis apparatus consisting of a gas supply part, an electrical heating reactor and a real-time data monitoring system, as shown in Figure 2. The gas supply part mainly provided the reaction atmosphere under a mixed composition of CO_2 and N_2 for the CCCR of the calcium-based absorbent. This part mainly included steel cylinders filled with CO_2/N_2, pressure-reducing valves, rotameters and gas supply pipes. The electrical heating reactor provided a stable temperature field for the cyclic calcination and carbonation reactions of the calcium-based absorbent particles to ensure that the CCCR was performed at the set temperature. The heating part mainly included an electric heater, a temperature controller and a thermocouple. The reaction part mainly included quartz tubes, crucibles and hanging wires. The real-time data monitoring system, which was mainly composed of an electronic balance and a computer, was used to accurately and effectively monitor and save the mass changes in the reactants.

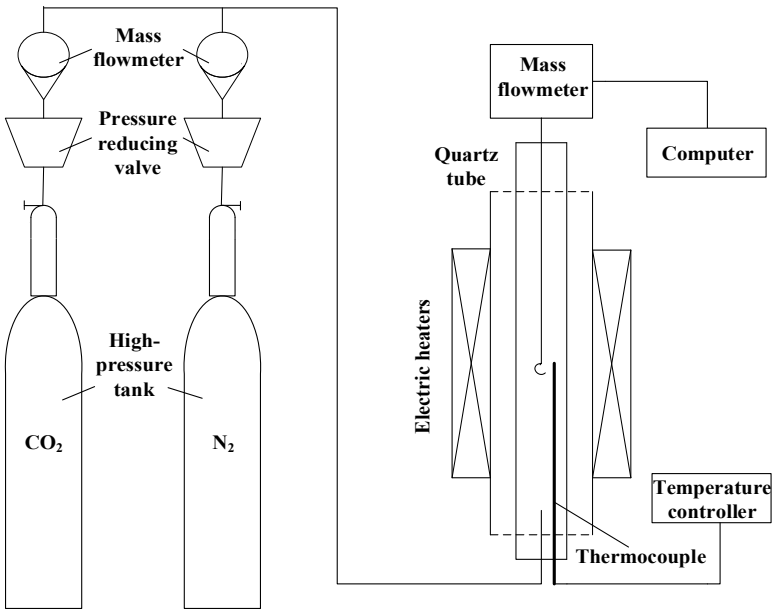

Figure 2. Schematic illustration of the experimental apparatus.

The weighing sensitivity of the experimental system was 0.1 mg, and the weighing range could be adjusted from 0 to 200 g. The temperature in the range of 0–1000 degrees Celsius could be measured, and the repeatability error was ±1%. During the experiment, the thermogravimetric data were automatically recorded and saved by the self-developed system software, and the time-conversion curves could be obtained by the subsequent data processing software. The atmosphere of the calcination reaction of the limestone particles was formed by nitrogen, and the atmosphere of the carbonation reaction was formed by the mixed gas of nitrogen and carbon dioxide; the portion of the former was 85%, and the portion of the latter was 15%. The proportions of the two kinds of gases were controlled by two rotary flowmeters. The purities of N_2 and CO_2 were both greater than 99.9%. It should be noted that the adsorption process was carried out under the condition of pure CO_2, while the calcination condition was carried out under the condition of pure N_2.

2.2. Experimental Materials

The experimental samples were made of natural limestone. After being crushed and sieved, the particle sizes of the limestone particles ranged from 48 μm to 62 μm. The limestone particles were dried to a constant weight at 105 °C before analysis, placed in a desiccator to be cooled to room temperature and finally sealed for storage. The chemical compositions contained in the limestone particles were measured by an X-ray atomic fluorescence spectrometer (XRF, EAGLE III type). The results are listed in Table 1.

Table 1. Chemical composition of the limestone particles (wt %).

CaO	MgO	SiO_2	Al_2O_3	Fe_2O_3	K_2O	TiO_2	Cr_2O_3	SrO	MnO	SO_3	LOI *
49.70	3.45	2.31	0.74	0.56	0.22	0.05	0.05	0.03	0.02	0.02	42.85

* LOI = loss on ignition.

3. Test and Analysis

3.1. Limestone CCCR Experimental Process

The experiment was carried out under normal pressure, and each time, samples of 0.2 ± 0.02 g were taken and laid flat in the crucible to form a thin layer with a uniform thickness in order to reduce the diffusion resistance between the sample particles. A higher reaction gas flow rate of 1000 mL/min was adopted during the calcination and carbonation so as to reduce the diffusion resistance between the reaction gas and particles. It should be pointed out that the flow rate selected in this paper is 2~5 times that of the minimum fluidization velocity of particles, and the gas flow rate in this range has little impact on the content of this study. The experimental process was maintained in isothermal conditions, i.e., the calcination temperature of the limestone particles was maintained at 900 °C, and the calcination temperature of the CaO particles was maintained at 700 °C so as to get closer to the real reaction processes. By preliminary experiments, the complete combustion duration and the full carbonation duration of the samples were determined, which were, respectively, 4 min and 15 min. In order to investigate the effects of excessive sintering that was caused by a prolonged calcination duration on the CO_2 absorption process of the calcium-based adsorbent, the effects of a calcination duration prolonged to 30 min in the first cycle and the effects of a calcination duration prolonged to 30 min in the third cycle were respectively analyzed by a comparison with the experimental data of a complete calcination duration of four minutes. In addition, in the calcination of the third cycle, the calcination temperature was increased to 950 °C to investigate the effects of excessive sintering caused by the increased calcination temperature on the CCCR process. During the experiment, the calcination of the limestone particles was firstly performed under the set calcination temperature and atmosphere. After the calcination process was finished, the reactor temperature was adjusted to the set carbonation temperature, and the carbonation of the CaO particles was performed under the corresponding atmosphere to complete a cycle.

3.2. Characterization Parameters

In order to visually compare the differences in the surface structures of the samples under different cycles, a scanning electron microscope (SEM, JSM-7500F) was used to magnify and analyze the sample morphologies.

The surface void structure of the samples with different calcination/carbonation times was determined by a TristarII3020 automatic surface area and porosity analyzer from Micromeritics, which was used to perform static isothermal adsorption measurements at liquid nitrogen saturation temperature (77 K, which is the operating temperature). The specific surface area of the samples was calculated by the BET method according to adsorption/desorption curves. The specific pore volume, pore volume distribution and surface area distribution of the samples were obtained by the BJH method.

3.3. Calculation of Carbonation Conversion

In the analysis of the experimental results, the conversion rate X is used to reflect the degree of CaO carbonation. The specific calculation method is shown as Equation (1):

$$X = \frac{M_{\mathrm{CaO}}(m_{N_t} - m_{N_0})}{M_{CO_2} m_0 A} \quad (1)$$

where X is the carbonation conversion rate of the CaO sample, %; m_0 is the initial mass of the sample, g; A is the content of CaO in the initial sample, %; m_{Nt} is the mass of the sample after t minutes of the Nth cyclic carbonation reaction, g; M_{CaO} and M_{CO2} are the molar masses of CaO and CO_2, respectively, g/mol; and m_{N0} is the mass of the sample after the Nth cycle of calcination, g. The mass of the sample after calcination in each cycle of the experiment is assumed to be basically the same as before the reaction.

4. Results and Discussion

4.1. Limestone Cycle Reaction Characteristics

Figure 3 shows the initial TGA curve of limestone after seven cycles of calcination/carbonation. In Figure 3, stage A represents the calcination and decomposition process of limestone at high temperature. Due to the release of a large amount of CO_2, the total mass of the limestone decreases rapidly. Stage B reflects the rapid carbonation process of the calcined product, which is mainly the absorption reaction of CaO to CO_2. The gas precipitation during the initial calcination makes the surface of CaO rich in micropores, which is conducive to the rapid diffusion of CO_2 and the interaction with CaO particles in the full reaction; therefore, at the beginning of the carbonation process, the TG curve is reflected as a rapid increase in sample mass. However, as the carbonation of the solid sample proceeds, $CaCO_3$ generated on the surface of the CaO particles blocks some of the pores and hinders the further carbonation reaction between CO_2 and CaO inside the pores, resulting in a significant decrease in the carbonation rate. At this moment, one cycle of CaO calcination/carbonation is over.

As the number of cycles increases, the absorption capacity of CaO for CO_2 decreases significantly. The relationship between the number of cycles and the degree of carbonation is shown in Figure 4. It can be observed in the figure that the initial stage of the reaction is the chemical reaction control stage where the reaction rate is very fast; then, the increased rate of the reaction conversion rate is significantly reduced, and finally, the change trend tends to be gentle, entering the product layer diffusion control stage [16]. It should be pointed out that, from the effect of over-sintering, the selection of seven cycles has met the requirements of this work.

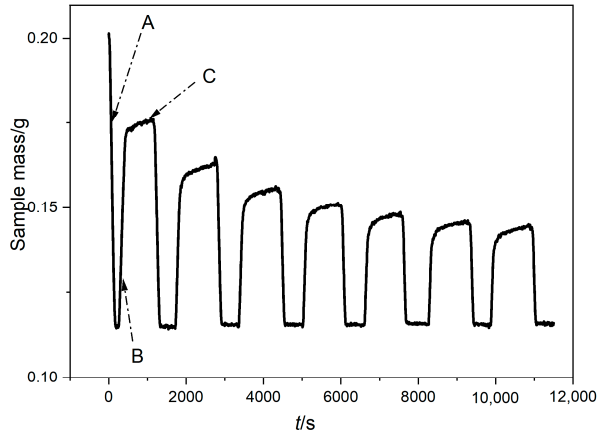

Figure 3. Initial TGA curve of limestone cyclic reaction.

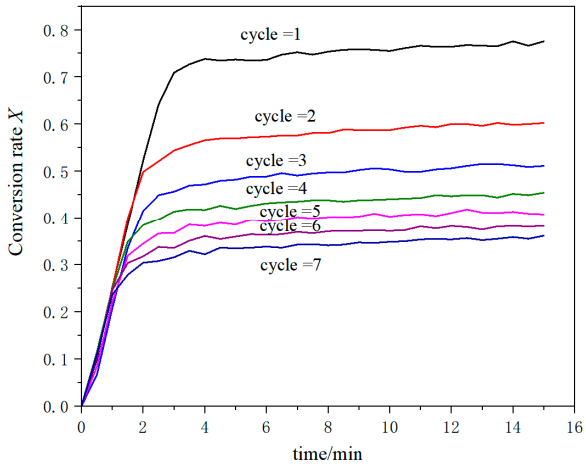

Figure 4. The relationship between the conversion rate of CaO cycle carbonation with time.

4.2. Effect of Sintering on CaO Final Conversion

Figure 5 reflects the effect of the sintering conditions on the final conversion of CaO at different cycles, where a represents the CCCR process of limestone within a certain complete calcination time; b represents the CCCR process of limestone in the first cycle of excessive sintering; c represents the CCCR process of limestone in the third cycle of excessive sintering; and d represents the CCCR process of excessive sintering of limestone to 950 °C in the third cycle.

It can be observed in Figure 6 that, with the increase in the number of cycles, the final conversion rate of CaO decreases under all four working conditions, and the decreasing trend is the most obvious in the previous four cycles. Under the b working condition, the final conversion rate of CaO in the first three cycles is less than that in the working condition; the first cycle has the largest decline, and then, the decline rate gradually decreases. Finally, the final conversion rate of CaO exceeds the a working condition after the fourth cycle. Under the conditions of c and a, the final conversion rate of CaO shows the same change trend with the number of cycles, indicating that excessive sintering in the third cycle has basically no effect on this cycle and subsequent cycles. However, the d working condition has a relatively large change compared with the a and c working conditions, that is, the final conversion rate of CaO in the third cycle rapidly attenuates and then gradually increases and exceeds the a and c working conditions. This indicates that the excessive sintering caused by the increase in calcination temperature is limited to this cycle, which has a certain promoting effect on the subsequent carbonation reaction.

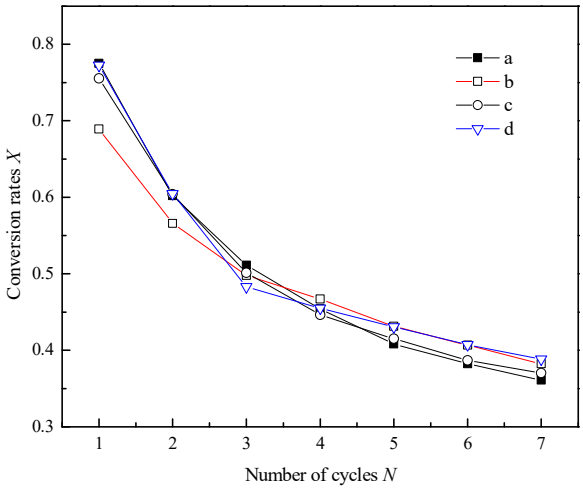

Figure 5. The relationship between the final conversion of CaO and the number of cycles under different sintering conditions.

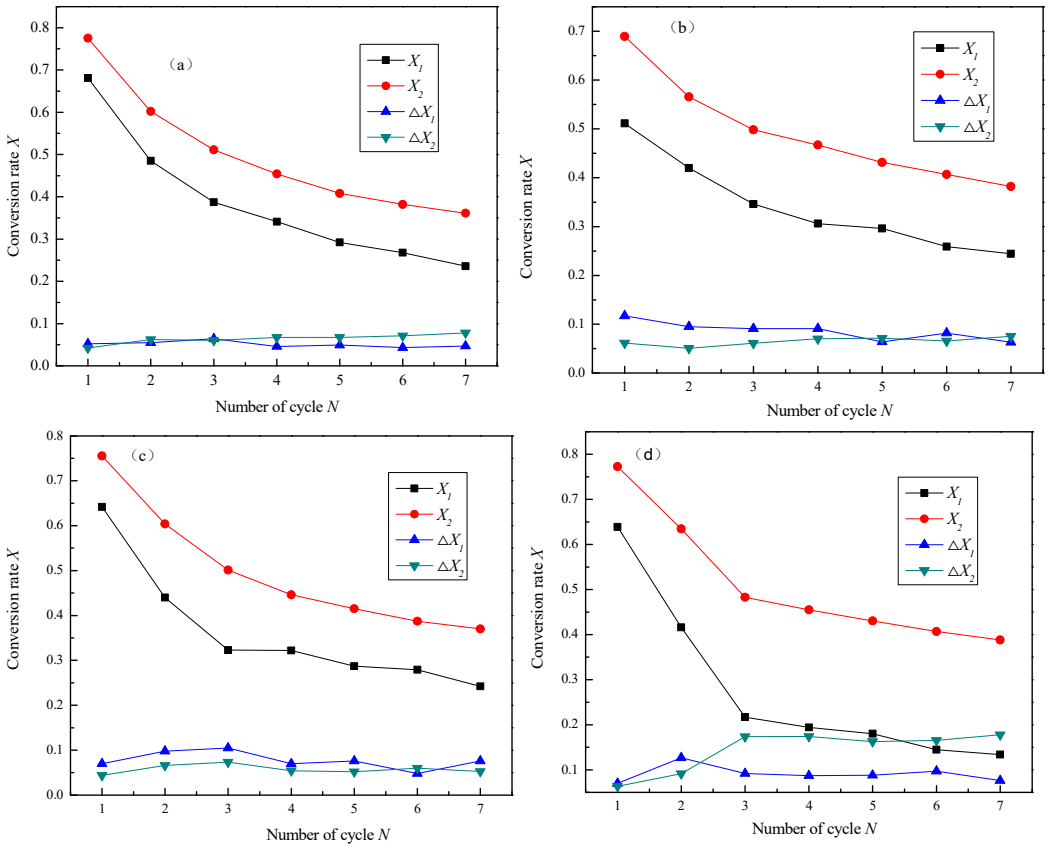

Figure 6. The relationship between the conversion rate of each reaction stage and the number of cycles under different sintering conditions (**a**–**d**).

4.3. Analysis of CaO Reactivity under Different Sintering Conditions

In order to further analyze the effect of different sintering conditions on the reduction in CaO reactivity, this section studies the variation in the CaO conversion rate with the number of cycles at different stages, which is shown in Figure 7.

In this figure, X_1 represents the conversion rate of CaO in the chemical reaction control stage; X_2 is the final conversion rate of the entire reaction stage; ΔX_1 is the conversion rate from the end of the chemical reaction control stage to the beginning of the product layer control stage; and ΔX_2 is the conversion rate from the beginning of the control stage of

the product layer to the final. It can be observed in Figure 6 that the final conversion rate of CaO is mainly composed of X_1, and ΔX_1 and ΔX_2 account for a relatively small share under a, b and c conditions. However, under the d condition, the final conversion rate of CaO mainly consists of X_1 in the first three cycles, and in the next four cycles, X_1 and ΔX_2 have basically the same share.

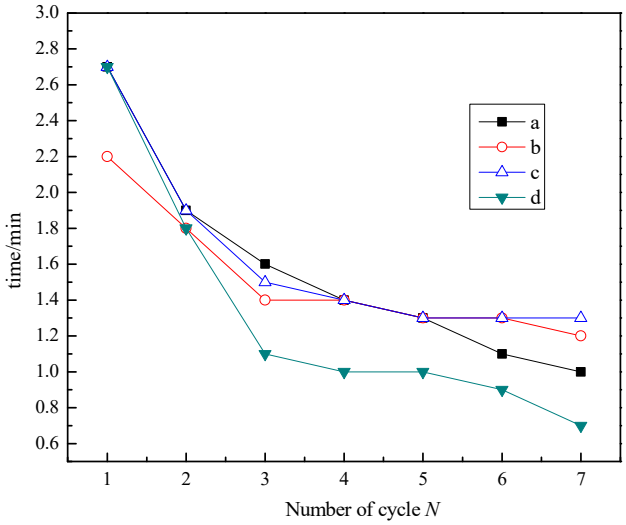

Figure 7. The relationship between the end time of the chemical reaction control stage and the number of cycles under different sintering conditions.

Comparing the changes in the curves in Figure 7, it can be observed that, under the four conditions, X_1 decreases with the increase in the number of cycles, but the trend of the change is different. Taking the a condition as a reference value, under the b working condition, X_1 is smaller, but as the number of cycles increases, the rate of decrease gradually slows down; the *c* condition decreases rapidly during the first three cycles, but the change in X_1 gradually decreases in the subsequent cycles. The change trend of X_1 under the d working condition is similar to that under the c working condition, except it decreases more significantly. In addition, the change in ΔX_1 is not obvious under the four conditions, and ΔX_2 only increases slightly under the d working condition. Overall, Figure 8 shows that the decrease in CaO reactivity is mainly caused by the decrease in X_1, and the different sintering conditions have different effects on the decrease in activity.

Further analysis revealed that the decline of X_1 is related to the early end of the chemical reaction control phase. As shown in Figure 8, the end times of the chemical reaction control stage under the four conditions all advance with the increase in the number of cycles, and the variation range is different under different sintering conditions. Among them, under the b condition, the end time of the first three cycles of the chemical reaction control phase is earlier than the a condition due to the excess sintering of the first cycle. The change trend of the *c* condition is basically the same as that of the a condition, while the d condition has a larger decline, and the end time of the chemical reaction control stage after the third cycle is far ahead of the a condition.

Based on the above research, it can be observed that the decrease in CaO activity under different sintering conditions mainly occurs in the chemical reaction control stage, while in the product layer diffusion control stage, the effect of sintering on the CaO conversion rate is small. This indicates that the excessive sintering of CaO particles mainly has a greater impact on the chemical reaction control stage but less of an impact on the product layer diffusion stage, which is related to the reaction mechanism in the different stages [20]. In addition, this study shows that the excessive sintering caused by prolonging the calcination time and increasing the calcination temperature has a greater impact on this cycle only, and the effect quickly weakens in subsequent cycles. It shows that the rapid reduction in

pore-specific surface area caused by the excessive sintering in the previous cycle will be recovered in the next cycle.

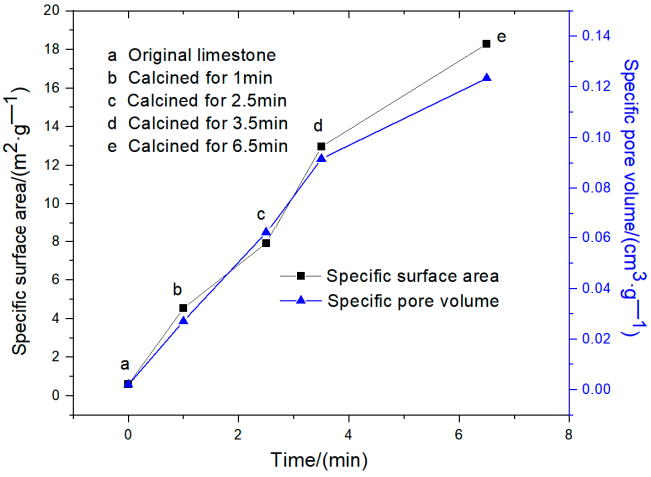

(**a**)

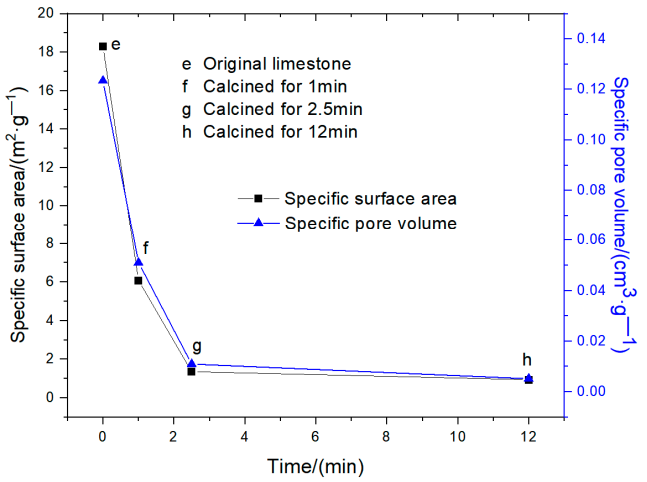

(**b**)

Figure 8. Specific surface area and pore volume of different procedural products derived from limestone. (**a**) Calcining process; (**b**) Carbonation process.

4.4. Specific Surface Area

Figure 8a–d and e represent the original limestone, calcined for 1 min, calcined for 2.5 min, calcined for 3.5 min, calcined for 3.5 min, calcined for 3.5 min, calcined for 2.5 min and calcined for 3.5 min. When calcined for 6.5 min, f, g and h represent that the calcined products of limestone are carbonated for 1 min, 2.5 min and 12 min, respectively. This representation method is also applicable to the analysis of the following chart.

The specific surface area and pore volume are typical parameters to characterize the microstructure of materials. In the process of calcination/carbonation of limestone, the composition of intermediate products is different, and its surface characteristics are also different. It can be observed in Figure 9 that the specific surface area and specific pore volume of the initial limestone are both small, and the calcination reaction causes the specific surface area and specific pore volume of the calcined products to increase linearly with the calcination time, while the carbonation reaction leads to the exponential and rapid decay of the specific surface area and specific pore volume of the carbonated products.

The large specific surface area and pore volume obtained are basically exhausted in the rapid reaction stage of carbonation. The specific changes are as follows. For limestone calcined for 1 min, the specific surface area and pore volume of the product increased 7.6 times and 13.7 times, respectively, compared with the initial limestone, while the specific surface area and pore volume of the product calcined for 2.5 min further increased 13.2 times and 31.6 times. Relatively speaking, the growth rate of the specific pore volume during calcination is faster than that of the specific surface area. When the limestone is calcined for 6.5 min, it completely decomposes, and no sintering occurs. At this time, the specific surface area and specific pore volume reach the maximums, which are 30.5 times and 62.7 times those of the original limestone, respectively.

When carbonated for 1 min, the specific surface area and pore volume of the carbonated products rapidly decreased to 0.33 times and 0.41 times the maximum values. After carbonation for 2.5 min, the specific surface area and pore volume of the product are basically exhausted and decay to 0.07 and 0.09 times the maximum values, respectively. When carbonation continues, the carbonation process gradually transitions to the diffusion control stage, and the carbonation conversion rate only increases by approximately 0.1 from 2.5 min to 12 min. The specific surface area and specific pore volume decay to 0.05 and 0.04 times the maximum values, but they are still 1.5 and 2.6 times those of the initial limestone. Therefore, with the continuation of carbonation time, the carbonation process can be improved. The conversion rate will continue to increase slowly to deplete the remaining specific surface area and pore volume.

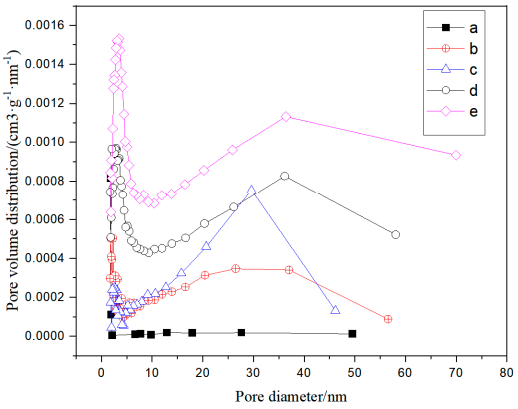

(**a**)

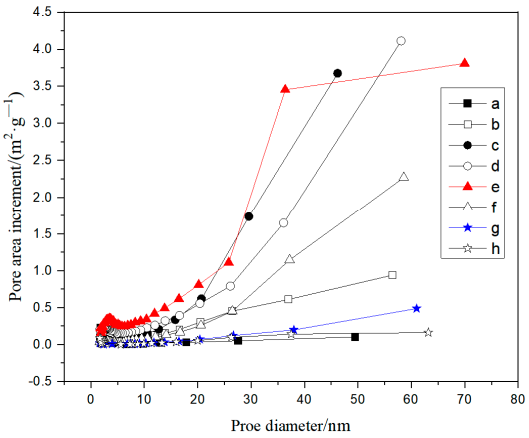

(**b**)

Figure 9. *Cont.*

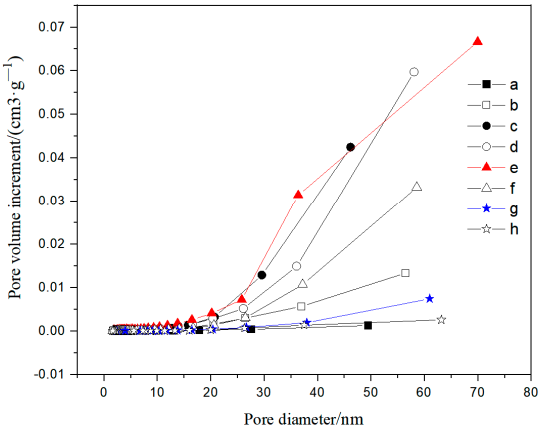

(**c**)

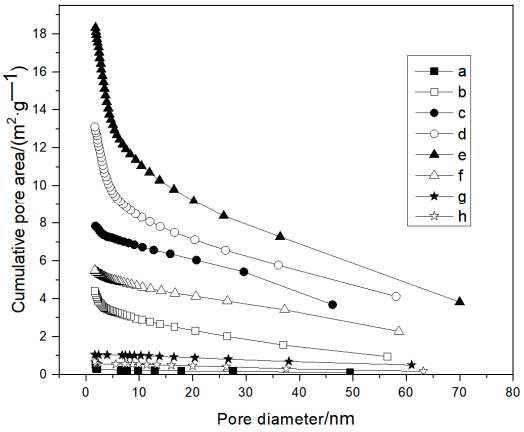

(**d**)

Figure 9. Pore distribution changes in products of limestone in different calcination/carbonation stages. (**a**) Pore volume distribution; (**b**) Pore volume increment; (**c**) Incremental pore area; (**d**) Cumulative pore area.

4.5. Pore Distribution

The pore distribution of the products in the process of calcination/carbonation of limestone includes pore area distribution and pore volume distribution, which show the pore area and pore volume occupied by different void sizes. The study of pore distribution can better show the changes in pore structure in the process of calcination/carbonation of limestone. According to IUPAC's classification of pore size, a pore size less than 2 nm is a micropore, a pore size between 2 and 50 nm is a mesopore, and a pore size greater than 50 nm is a macropore [21]. A micropore provides a huge inner surface for the reaction, a middle pore is the main channel into a micropore, and a large pore is a rough channel for transporting the reaction component.

As shown in Figure 9, the pore distribution of the calcined/carbonated products changes regularly with the progress of the calcined/carbonated reaction. As can be observed in Figure 9a, the original limestone is basically non-porous, so its specific surface area and specific pore volume are very small. After 1 min of calcination, the double peaks were prominent, and micropores, medium pores and large pores appeared, but the total number of the three kinds of pores was small, so the specific surface area and specific pore volume of the calcined products were still small at this time. After calcination for

2.5 min, the first peak changed little, but the peak value of the second peak increased rapidly, indicating that the middle pore formed sharply and promoted the ratio table.

The area and specific pore volume increased further, and the rapid formation of the mesopore during the calcination is the main reason for the faster growth of the specific pore volume and specific surface area. Calcined to 6.5 min, the limestone completely decomposed, and a CaO void basically formed, mainly composed of medium and large pores, with a certain amount of micropores.

The pore volume distribution shows a bimodal structure: the first peak is distributed in 1.7~10 nm, the second peak is distributed in 10~80 nm, and the peak value reaches the maximum, while the specific surface area and specific pore volume also reach the maximum. After carbonation for 1 min, the peak value of both peaks decreased sharply, and the remaining void was similar to that of the calcined products for 1 min, with a small number of pores. After carbonation for 2.5 min and 12 min, the pore volume distribution of the carbonated products was basically the same, and the micropores basically disappeared, leaving only a very small number of medium pores and large pores.

Figure 9b,c reflect the extent to which the different types of pores contribute to the volume and area of the pore. With the calcination reaction of limestone, micropores have little contribution to the increase in pore volume but have a certain contribution to the increase in pore area. The contribution of medium and large pores to the volume and area of the pore is greater. The carbonation reaction is the reverse reaction of the calcination reaction, and the pore volume and pore area obtained by the calcination reaction are consumed in the process of the carbonation reaction. As shown in Figure 9b,c, with the progress of the carbonation reaction, the pore volume and area contributed by micropores, mesoporous pores and macropores are consumed at the same time, and when the reaction becomes stable, the pore volume and area are almost consumed. Figure 9d shows the cumulative pore area when the pore size changes. The pore area increases continuously during calcination, while the pore area decreases continuously during carbonation. The steep curve at the pore area further indicates that the pore area has a greater influence on the increase in pore area.

4.6. Surface Morphology Analysis of the 7th Calcined Product

The adsorption reaction mainly depends on the specific surface area of the adsorbent, and the size of the specific surface area is mainly affected by the pore structure. In this section, the scanning electron microscopy method was used to obtain the pore distribution characteristics of the calcined product as shown in Figure 10. Figure 10 is the scanning electron microscope analysis of the 7th calcined product. Under a magnification of 5000 times, it can be clearly observed that the calcined product is in a porous state; after a further magnification of 10,000 times, it can be found that the calcined product has a multi-layer structure, and CO_2 needs to penetrate the pores during the adsorption process and enter the interior of the calcined product to increase adsorption. Under a magnification of 20,000 times, it can be found that the pores are mainly small pores, and the connectivity between the pores is poor due to the influence of sintering; after a magnification of 50,000 times, the collapse and fusion of the pores caused by sintering are more obvious [22,23].

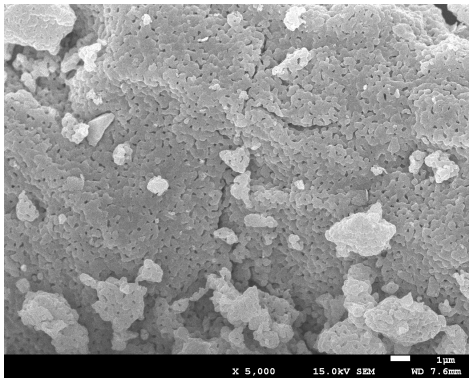

(**a**)

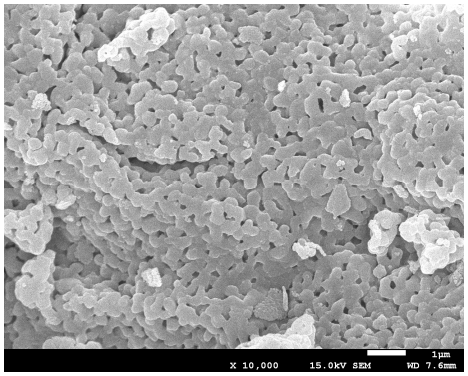

(**b**)

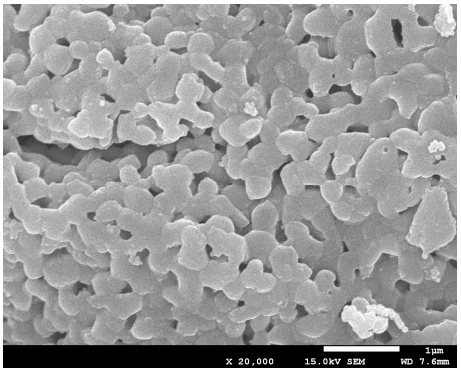

(**c**)

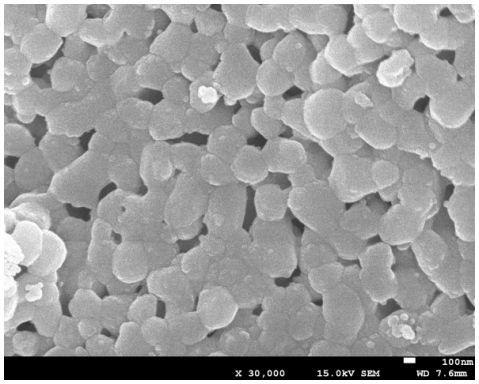

(**d**)

Figure 10. The product surface morphology under the 7th calcined product. (**a**) Magnify 5000 times; (**b**) Magnify 10,000 times; (**c**) Magnify 20,000 times; (**d**) Magnify 30,000 times.

5. Conclusions

By prolonging the calcination time and increasing the calcination temperature, the limestone calcination process was over-sintering, and the effect of over-sintering on the characteristics of the Ca-based adsorbent cycle CO_2 separation process was studied. The following conclusions were obtained:

(1) The excessive sintering caused by prolonging the calcination time and increasing the calcination temperature has a greater inhibitory effect on the current cycle only, and this inhibitory effect quickly weakens in subsequent cycles. With the further increase in the number of cycles, the excessive sintering in the early stage can improve the subsequent carbonation reaction to a certain degree.

(2) Both the specific surface area and specific pore volume of limestone are small before calcination, and the calcination reaction causes the specific surface area and specific pore volume of the calcined products to increase linearly with the calcination time, while the carbonation reaction results in the exponential rapid decay of the specific surface area and specific pore volume of the carbonated products, and the large specific surface area and specific pore volume obtained by calcination are basically depleted in the rapid reaction stage of carbonation.

(3) The pore volume distribution curve of the completely decomposed products of limestone presents a bimodal structure, with the first peak distributed within 1.7 nm~10 nm and the second peak distributed within 10 nm~80 nm. In the early stage of calcination, the double peaks are prominent. With the continuation of calcination, the peak value of the double peaks increases continuously, and the peak value reaches the maximum when the calcination is complete, and no sintering is produced. The carbonation reaction caused the sharp reduction in the peak value of the double peaks, and the double peaks basically disappeared after 2.5 min. The contribution of micropores, medium pores and large pores to the increase in pore volume and area is different. Micropores only contribute to the increase in pore area, while medium and large pores both contribute to the pore volume and area.

Author Contributions: Conceptualization, J.C. and H.J.; methodology, J.W.; software, X.Y.; validation, J.C., J.W. and X.Z.; formal analysis, X.Z.; investigation, J.W.; resources, J.C.; data curation, J.C.; writing—original draft preparation, J.W.; writing—review and editing, H.J.; visualization, J.C.; supervision, J.C.; project administration, J.C.; funding acquisition, J.C. All authors have read and agreed to the published version of the manuscript.

Funding: This research was funded by the Research Project of Science and Technology Department of Henan Province (242102240093, 242102240124), Key Scientific Research Project of Education Department of Henan Province (24B480015), and Research Project of Zhengzhou Electric Power College (ZEPCKY2021-14, ZEPCKY2023-02, ZEPCKY2024-3). Supported by: Youth Fund of Natural Science Foundation of Hebei Province (E2020502007); General Project Funding of Central University Fund Project (2020MS103).

Data Availability Statement: No new data were created or analyzed in this study.

Conflicts of Interest: The authors declare no conflict of interest.

Nomenclature

X	the carbonation conversion of the CaO sample
m_0	the initial mass of the sample, g
A	the content of CaO in the initial sample, g
N	the cycle number
m_{N_t}	the mass of the sample after t min of the Nth cyclic carbonation reaction, g
m_{N_0}	the mass of the sample after the Nth cycle of calcination, g
M_{CaO}	the molar masses of CaO, g/mol
M_{CO_2}	the molar masses of CO_2, g/mol
t	time, min

References

1. Huang, Z.; Xie, X.; Zhang, T. Medium- and Long-Term Energy Demand of China and Energy Transition Pathway Toward Carbon Neutrality. *Strateg. Study CAE* **2022**, *24*, 8–18. [CrossRef]
2. Shu, Y.B.; Zhang, L.Y.; Zhang, Y.Z.; Wang, Y.H.; Lu, G.; Yuan, B.; Xia, P. Carbon peak and carbon neutrality path for China's power industry. *Strateg. Study CAE* **2021**, *23*, 1–14. [CrossRef]
3. Yu, B.; Zhao, G.; An, R.; Chen, J.; Tan, J.; Li, X. Research on China's CO_2 emission pathway under carbon neutral target. *J. Beijing Inst. Technol. (Soc. Sci. Ed.)* **2021**, *23*, 17–24.
4. Zhang, X.; Li, Y.; Ma, Q.; Liu, L. Development of carbon capture, utilization and storage technology in China. *Strateg. Study CAE* **2021**, *23*, 70–80. [CrossRef]
5. Wei, N.; Jiang, D.L.; Liu, S.N. Cost competitiveness analysis of CCUS transformation of coal-fired power plants of National Energy Group. *Proc. Chin. Soc. Electr. Eng.* **2020**, *40*, 1258–1265.
6. Jiang, Y.; Lei, Y.L.; Yan, X. Employment impact assessment of carbon capture and storage (CCS) in China's power sector based on input-output model. *Environ. Sci. Pollut. Res.* **2019**, *26*, 15665–15676. [CrossRef] [PubMed]
7. Zhang, X.; Li, K.; Ma, Q.; Fan, J.L. Orientation and prospect of CCUS development under carbon neutrality target. *China Popul. Resour. Environ.* **2021**, *31*, 29–33.
8. Wang, Y.; Pan, Z.; Zhao, Y.; Luo, Y.; Gao, X. Research progress in CO_2 solid sorbents for hydrogen production by sorption-enhanced steam reforming: A review. *Chem. Ind. Eng. Prog.* **2019**, *38*, 5103–5113.
9. Li, Y.; Zhang, Y.; Chen, X.L.; Gong, X. Effect of cyclic adsorption performance of calcium-based sorbent on enhanced biomass gasification for hydrogen production. *CIESC J.* **2020**, *71*, 777–787.
10. Wang, Y. *Experimental Studies on Sorption Enhanced Ethanol Steam Reforming for H2 Production with Modified CaO-Based Sorbents*; Dalian University of Technology: Dalian, China, 2022.
11. Shimizu, T.; Hirama, T.; Hosoda, H.; Kitano, K.; Inagaki, M.; Tejima, K. A twin fluid-red reactor for removal of CO_2 from combustion processes. *Chem. Eng. Res. Des.* **1999**, *77*, 62–68. [CrossRef]
12. Chen, H.W.; Chen, J.T.; Wei, R.G.; Chen, L. Compensation effect in kinetics of Ca-based absorbents calcination reaction at different temperature. *J. Cent. South Univ. (Sci. Technol.)* **2013**, *44*, 2165–2170.
13. Li, Y.; Zhao, C.S. Carbonation Characteristics in calcium sorbents cyclic calcination/carbonation reaction process. *Proc. CSEE* **2008**, *28*, 55–60.
14. Sun, S.; Wang, Y.; Xu, Y.; Sun, H.; Zhao, X.; Zhang, Y.; Yang, X.; Bie, X.; Wu, M.; Zhang, C.; et al. Ni-functionalized Ca@Si yolk-shell nanoreactors for enhanced integrated CO_2 capture and dry reforming of methane via confined catalysis. *Appl. Catal. B Environ. Energy* **2024**, *348*, 123838. [CrossRef]
15. Xu, Y.; Wu, M.; Yang, X.; Sun, S.; Li, Q.; Zhang, Y.; Wu, C.; Przekop, R.E.; Romańczuk-Ruszuk, E.; Pakuła, D.; et al. Recent advances and prospects in high purity H_2 production from sorption enhanced reforming of bio-ethanol and bio-glycerol as carbon negative processes: A review. *Carbon Capture Sci. Technol.* **2023**, *8*, 100129. [CrossRef]
16. Xu, Y.; Luo, C.; Sang, H.; Lu, B.; Wu, F.; Li, X.; Zhang, L. Structure and surface insight into a temperature-sensitive CaO-based CO_2 sorbent. *Chem. Eng. J.* **2022**, *435*, 134960. [CrossRef]
17. Xu, Y.; Donat, F.; Luo, C.; Chen, J.; Kierzkowska, A.; Naeem, M.A.; Zhang, L.; Müller, C.R. Investigation of K_2CO_3-modified CaO sorbents for CO_2 capture using in-situ X-ray diffraction. *Chem. Eng. J.* **2023**, *453*, 139913. [CrossRef]
18. Xu, Y.; Lu, B.; Zhang, Z.; Luo, C.; Zhang, L.; Zheng, C. Cyclic CO_2 Capture Characteristics of the K Modifified Ca-based Sorbent. *J. Eng. Thermophysics.* **2022**, *43*, 2106–2110.
19. Kuang, S.; Chen, W.; Wen, S.; Lin, W.; Wang, A.; Liu, S.; Tian, C. Enhanced Adsorption of CO_2 by Mg/Y modified Ca-based adsorbents. *Clean Coal Technol.* **2022**, *28*, 195–202.
20. Li, Z.; Cai, N.; Zhao, X.; Huang, Y. Kinetic characteristic of the multiple carbonation cycle reactions of CaO with CO_2. *J. Combust. Sci. Technol.* **2006**, *12*, 481–485.
21. Xu, R.; Pang, W. *Chemistry of Molecular Sieve and Porous Materials*; Science Press: Beijing, China, 2004; pp. 145–148.
22. Chen, J.; Wei, R.; Chen, H.; Chen, L. Activity decline analysis of the cyclic CO_2 capture using limestone. *Electr. Power Sci. Eng.* **2012**, *28*, 42–46.
23. Chen, J. *Study on Characteristics of Kinetics and Variation Behavior of Microstructure during Ca-Based Absorbents CCCR Process*; North China Electric Power University: Beijing, China, 2013.